

The pomeron-pomeron interaction in the perturbative QCD

N.Arместо and M.A. Braun*

Departamento de Física de Partículas,
Universidade de Santiago de Compostela,
15706-Santiago de Compostela, Spain

June 1996

Abstract

The pomeron-pomeron interaction is studied in the perturbative approach of BFKL-Bartels. The total pomeron-pomeron cross-section is proportional to $\alpha_s^4 s^\Delta / \sqrt{t_1 t_2}$ where \sqrt{s} is the c.m. energy and $t_{1,2}$ are the virtualities of the colliding pomerons. Upon calculating the coefficient the cross-section is found to be of the order 2.2 mb at $\sqrt{s} = 6$ TeV and $\sqrt{-t_1} \sim \sqrt{-t_2} \sim 1$ GeV/c.

US-FT/27-96
hep-ph/9606307

*Visiting professor IBERDROLA. Permanent address: Department of High-Energy Physics, University of St. Petersburg, 198904 St. Petersburg, Russia.

1 Introduction

The study of high-mass diffractive events brings into consideration properties of the pomeron (P), which may be pragmatically associated with a high-mass object appearing between the rapidity gaps. In particular, diffractive events in DIS allow to study the structure function of the pomeron and central diffractive events in hadronic or photonic collisions reveal the properties of the PP interaction. Most of the theoretical activity in this domain has concentrated on the problem of extracting the pomeron properties from the data, rather than to study these properties themselves.

Such a study is possible in the perturbative framework of the "hard pomeron", in which the realistic QCD is modified by introducing an infrared cutoff (e.g. via the Higgs mechanism) and subsequently fixing a (small) coupling constant. As is well known, this theory results infrared stable in the colourless sector, so that one might think that at least part of its predictions remain valid for the realistic QCD.

In a recent publication [1], in this approach, we have studied the triple pomeron interaction, which is vital for the pomeron structure function. The present note extends this study to a more complicated case of the PP scattering cross-section, which evidently involves two triple pomeron vertices.

Since the hard pomeron theory is scale invariant, the dependence of the PP scattering cross-section on the relevant variables is trivially predicted in this theory. If the two colliding pomerons have their momenta l and l' with $t_1 = l^2 < 0$ and $t_2 = l'^2 < 0$, and their c.m. energy squared is $s = (l + l')^2$, then from dimensional considerations and properties of the BFKL pomeron [2] one finds for the total PP cross-section

$$\sigma_{PP}^{tot}(s, t_1, t_2) = c \frac{\alpha_s^4 s^\Delta}{\sqrt{at_1 t_2 \ln s}}. \quad (1)$$

Here the pomeron intercept Δ and the parameter a are known functions of the strong coupling constant α_s (see Eq. (18)) and c is an unknown number. Therefore the problem of studying the PP cross-section reduces to finding the numerical constant c in (1). One should have in mind that this constant factor is in fact rather ill-defined. On the one hand, the separation of the PP cross-section from the rest of the amplitude inevitably involves a certain arbitrariness, known as a choice of the "flux factor" [3]. In the hard pomeron theory, as we shall see, this problem is aggravated because the pomeron coupling to external sources results singular for small momentum transfers. On the other hand, the scale of $\ln s$ in the hard pomeron approach remains arbitrary, which introduces an undetermined factor in (1).

In the following we calculate the coefficient c within a certain (rather obvious) choice of the flux factor and neglecting the numerical factor which comes from s^Δ in (1). This latter

approximation corresponds to the (theoretically justified) assumption of a very small Δ . In applications we take the scale involved of the order of 1 GeV², as favoured by the pomeron phenomenology. Our calculations give a rather large value for c :

$$c \simeq 35370. \quad (2)$$

Possible experimental consequences of this result are discussed in Section 4 of this note. Sections 2 and 3 are dedicated to its derivation.

2 The central diffraction cross-section

The PP cross-section enters as a part of a more general central diffraction cross-section in which the colliding hadrons (or photons) produce a high mass M in the central region separated from the target and projectile by large rapidity gaps (Fig. 1). As seen from this figure, both projectile and target emit pomerons with momenta l and l' , respectively, which interact in the central part of the diagram. We introduce the standard energetic variables (see Fig. 1 for the notation of the momenta involved)

$$s = (p_1 + p_2)^2, \quad s_{12} = (p_1 + l')^2, \quad s_{21} = (p_2 + l)^2, \quad M^2 = (l + l')^2, \quad (3)$$

constrained by the relation

$$s_{12}s_{21} = sM^2. \quad (4)$$

We assume that all these variables are large with $s \gg s_{12}, s_{21} \gg M^2$. We also introduce

$$s_1 = s_{21}/M^2, \quad s_2 = s_{12}/M^2, \quad (5)$$

which serve as energetic variables for the upper and lower pomerons in Fig. 1, respectively.

In the hard pomeron approach the pomerons which connect the central part of Fig. 1 with the target and projectile are identified as BFKL pomerons. As to the central part itself, it is also given by a BFKL pomeron coupled to the upper and lower pomerons by two Bartels vertices $K_{2 \rightarrow 4}$, which describe transition of two reggeized gluons into four [4] (see Fig. 2). Explicitly the upper vertex $K_{2 \rightarrow 4}$, apart from a colour factor and a factor g^4 , is given by

$$K_{2 \rightarrow 4}(q_1, -q_1; q_2, l - q_2, -l + q_3, -q_3) \equiv K_l(q_1, q_2, q_3) = \frac{q_1^2 q_2^2}{(q_1 - q_2)^2} + \frac{q_1^2 q_3^2}{(q_1 - q_3)^2} - \frac{q_1^4 (q_2 - q_3)^2}{(q_1 - q_2)^2 (q_1 - q_3)^2}. \quad (6)$$

The lower vertex has the same form with the primed momenta.

Then we obtain the expression for the absorptive part D corresponding to Fig. 1 in the form

$$D = (1/16)g^{16}N^4(N^2 - 1)(s^2/M^2)(2\pi)^{-12} \int \prod_{i=1}^3 (d^2 q_i d^2 q'_i) K_l(q_1, q_2, q_3) K_{l'}(q'_1, q'_2, q'_3)$$

$$\phi_1(s_1, l, q_2)\phi_1(s_1, -l, -q_3)\phi_2(s_2, l', q'_2)\phi_2(s_2, -l', -q'_3)G(M^2, 0, q_1, -q'_1). \quad (7)$$

Here $\phi_{1(2)}(s, l, q)$ is a pomeron (a solution to the BFKL equation) coupled to the projectile (target) colourless external source with energy squared s , total momentum l and one of the gluon's momentum q . The function $G(M^2, 0, q_1, q'_1)$ is the BFKL Green function for the energy squared M^2 , total momentum zero and initial and final momentum of one of the gluons q_1 and q'_1 , respectively. It is assumed that the colour factor for each source is $(1/2)\delta_{ab}$ and that each source is proportional to g^2 . The factor $(1/16)N^4(N^2 - 1)$ comes from the colour variables, N being the number of colours ($N = 3$ for the physical QCD). Our normalization is that the double inclusive cross-section described by Fig. 1 is given by

$$\frac{d\sigma}{dt_1 dt_2 ds_{12} ds_{21}} = \frac{D}{256\pi^4 s^3}. \quad (8)$$

Since for $l \neq 0$ the solution of the BFKL equation is easier to obtain in the (transversal) coordinate space, we pass to this space by presenting

$$\phi(s, l, q) = \int d^2r \phi(s, l, r) \exp[i\mathbf{r}(q - l/2)]. \quad (9)$$

Evidently r is the transversal distance between the gluons. Then (7) transforms into

$$D = (1/16)g^{16}N^4(N^2 - 1)(s^2/M^2) \int \prod_{i=1}^3 (d^2r_i d^2r'_i) K_l(r_1, r_2, r_3) K_{l'}(r'_1, r'_2, r'_3) \\ \exp[-il(r_2 + r_3)/2 - il'(r'_2 + r'_3)/2] \\ \phi_1(s_1, l, r_2)\phi_1(s_1, -l, -r_3)\phi_2(s_2, l', r'_2)\phi_2(s_2, -l', -r'_3)G(M^2, 0, r_1, -r'_1), \quad (10)$$

where the 2 to 4 reggeon vertex in the coordinate space is obtained from (6) to be

$$K_l(r_1, r_2, r_3) = -2 \left[\delta^2(r_2)\delta^2(r_3)\nabla_1^2\delta^2(r) + \frac{1}{2\pi}\delta^2(r_3)r_2^{-2}(r_2\nabla_1)\nabla_1^2\delta^2(r) + \right. \\ \left. \frac{1}{2\pi}\delta^2(r_2)r_3^{-2}(r_3\nabla_1)\nabla_1^2\delta^2(r) + \frac{1}{(2\pi)^2}r_2^{-2}r_3^{-2}(r_2r_3)\nabla_1^4\delta^2(r) \right], \quad (11)$$

with $r = r_1 + r_2 + r_3$. The solutions ϕ vanish when $r = 0$. So only the last term in (11) survives. We then can rewrite (10) as

$$D = (1/4)g^{16}N^4(N^2 - 1)(s^2/M^2)(2\pi)^{-8} \\ \int d^2q d^2q' \chi(M^2, q + l/2, q' + l'/2) [\nabla_q \chi_1(s_1, l, q)]^2 [\nabla_{q'} \chi_2(s_2, l', q')]^2, \quad (12)$$

where

$$\chi(s, q, q') = \int d^2r d^2r' \exp(iqr + iq'r') \nabla^4 \nabla'^4 G(M^2, 0, r, -r') \quad (13)$$

and

$$\chi_{1,2}(s, l, q) = \int d^2r r r^{-2} \phi_{1,2}(s, l, r) \exp(iqr). \quad (14)$$

To calculate the function $\chi(s, q, q')$ we first integrate by parts in (13) to remove the derivatives,

$$\chi(s, q, q') = (qq')^4 \int d^2r d^2r' G(M^2, 0, r, -r') \exp(iqr + iq'r'). \quad (15)$$

The BFKL Green function at $l = 0$ and large s is given by the expression [5]

$$G(s, 0, r, -r') = \frac{1}{32\pi^2} r r' \int_{-\infty}^{\infty} \frac{d\nu s^{\omega(\nu)}}{(\nu^2 + 1/4)^2} (r/r')^{-2i\nu}, \quad (16)$$

where

$$\omega(\nu) = (g^2 N/2\pi^2) [\psi(1) - \text{Re}\psi(1/2 + i\nu)]. \quad (17)$$

Small values of ν play the dominant role in (16) at large s , so that we can approximate

$$\omega(\nu) = \Delta - a\nu^2; \quad \Delta = (g^2 N/\pi^2) \ln 2, \quad a = (7g^2 N/2\pi^2) \zeta(3). \quad (18)$$

Calculating the integrals over r and r' in (15) and then the remaining integral over ν we obtain

$$\chi(s, q, q') = 2qq' s^\Delta \sqrt{\frac{\pi}{a \ln s}} \exp\left(-\frac{\ln^2(q/q')}{a \ln s}\right). \quad (19)$$

At large s the exponential factor in (19) can evidently be neglected.

Now we turn to the functions $\chi_{1,2}(s, l, q)$. The solutions $\phi_{1(2)}$ can be obtained by using the Green function of the BFKL equation for a given total momentum $G(s, l, r, r')$. Following [6] and taking into account that the Green function G vanishes if r or r' are equal to zero and is isotropic at high energies one finds for, say, the projectile:

$$\phi_1(s, l, r) = -2 \int d^2\tilde{r} G(s, l, r, \tilde{r}) \rho_1(l, \tilde{r}) \exp(i\tilde{r}l/2). \quad (20)$$

Here $\rho_1(l, r)$ is the colour density of the projectile as a function of the intergluon distance r with the colour factor $(1/2)\delta_{ab}$ and g^2 separated. The explicit form of ρ can easily be found if the projectile is a highly virtual photon. For the longitudinal photon then

$$\rho_1^{(L)}(r) = \frac{4e^2 |p_1^2|}{(2\pi)^3} \sum_{f=1}^{N_f} Z_f^2 \int_0^1 d\alpha [\alpha(1-\alpha)]^2 K_0^2(\epsilon_f r) \exp(-i\alpha l r), \quad (21)$$

where $\epsilon_f^2 = |p_1^2| \alpha(1-\alpha) + m_f^2$ and m_f and Z_f are the mass and charge of the quark of flavour f , respectively. For the transverse photon a slightly more complicated formula emerges

$$\rho_1^{(T)}(r) = \frac{e^2}{(2\pi)^3} \sum_{f=1}^{N_f} Z_f^2 \int_0^1 d\alpha$$

$$\left\{ m_f^2 K_0^2(\epsilon_f r) + [\alpha^2 + (1-\alpha)^2] \epsilon_f^2 K_1^2(\epsilon_f r) - \alpha(1-\alpha)(1-2\alpha) K_0(\epsilon_f r) i l \nabla_r K_0(\epsilon_f r) \right\} \exp(-i\alpha l r). \quad (22)$$

Eqs (21), (22) generalize the well-known formulas for zero momentum transfer [6]. For a hadron projectile or target the form of the density is, of course, unknown, although one expects that it should be less singular at $r = 0$ and normalizable.

The leading contribution to the BFKL Green function at $l \neq 0$ has the form [5]

$$G_l(s, r, r') = \frac{1}{(2\pi)^4} \int \frac{d\nu \nu^2}{(\nu^2 + 1/4)^2} s^{\omega(\nu)} E_l^\nu(r) E_l^{-\nu}(r'), \quad (23)$$

where

$$E_l^\nu(r) = \int d^2 R \exp(ilR) \left(\frac{r}{|R + r/2||R - r/2|} \right)^{1+2i\nu}. \quad (24)$$

It is evident that the Green function (23), transformed into momentum space, contains terms proportional to $\delta^2(l/2 \pm q)$, which should be absent in the physical solution (this circumstance was first noted by A.H.Mueller and W.-K.Tang [7]). For that, (23) goes to zero at $r = 0$. Terms proportional to $\delta^2(l/2 + q)$ are not dangerous to us: they are killed by the vertex $K_{2 \rightarrow 4}$. To remove the dangerous singularity at $q = l/2$ and simultaneously preserve good behaviour at $r = 0$ we therefore make a subtraction in E , changing it to

$$\tilde{E}_l^\nu(r) = \int d^2 R \exp(ilR) \left[\left(\frac{r}{|R + r/2||R - r/2|} \right)^{1+2i\nu} - |R + r/2|^{-1-2i\nu} + |R - r/2|^{-1-2i\nu} \right]. \quad (25)$$

This subtraction removes the δ singularity at $q = l/2$ and doubles the one at $q = -l/2$, the latter eliminated by the kernel $K_{2 \rightarrow 4}$.

Integration over r in (14) leads to the integral

$$J(l, q) = \int (d^2 r / (2\pi)^2) (1/r^2) \tilde{E}_l^\nu(r) \exp(iqr). \quad (26)$$

This integral is convergent at any values of ν , the point $\nu = 0$ included, when the convergence at large values of r and R is provided by the exponential factors. So in the limit $s \rightarrow \infty$, when small values of ν dominate, we can put $\nu = 0$ in J :

$$J(l, q) = \int (d^2 R d^2 r / (2\pi)^2) \frac{\exp(ilR + iqr)}{r |R + r/2||R - r/2|} + (1/l) \ln \left(\frac{|l/2 - q|}{|l/2 + q|} \right). \quad (27)$$

The second term comes from the subtraction terms in (25). Passing to the Fourier transform of the function $1/r$ one can represent (27) as an integral in the momentum space

$$J(l, q) = (1/l) \int \frac{d^2 p (l + |l/2 + p| - |l/2 - p|)}{(2\pi) |l/2 + p| |l/2 - p| |q + p|}. \quad (28)$$

In the same manner we can put $\nu = 0$ in the function $E_l^{-\nu}(\tilde{r})$ obtaining for the integral over the transverse dimensions of the projectile

$$\int \frac{d^2 R d^2 r \exp[i l(R + r/2)] r \rho_1(l, r)}{|R + r/2||R - r/2|} = \pi R_1 F_1(t_1). \quad (29)$$

Here we have separated the characteristic transverse dimension of the projectile

$$R_1 = \int d^2r r \rho_1(0, r) \quad (30)$$

(and a factor π for convenience) and introduced a dimensionless function $F_1(t_1)$, which is a vertex for the interaction of the projectile with a pomeron at momentum transfer $\sqrt{-t_1} = l$. $F_1(t_1)$ behaves like $\ln|t_1|$ at small t_1 . The rest of the Green function is easily calculated by the stationary point method to finally give

$$\chi_1(s, l, q) = -\frac{4s^\Delta}{\sqrt{\pi}(a \ln s)^{3/2}} R_1 F_1(t_1) J(l, q). \quad (31)$$

Evidently the function $\chi_2(s, l, q)$ is given by the same formula with the projectile form-factor F_1 substituted by the target one F_2 .

Combining our results for χ and $\chi_{1,2}$, we obtain our final expression for the absorptive part D corresponding to the central diffraction from Eq. (12) to be

$$D = 8\pi^{-11/2} g^{16} N^4 (N^2 - 1) (s^2/M^2) \frac{(s_1^2 s_2^2 M^2)^\Delta}{\sqrt{a \ln M^2} (a \ln s_1)^3 (a \ln s_2)^3} [R_1 R_2 F_1(t_1) F_2(t_2)]^2 B^2 / \sqrt{t_1 t_2}. \quad (32)$$

Here the number B is defined as a result of the q integration

$$B = l \int (d^2q / (2\pi)^2) |l/2 + q| [\nabla_q J(l, q)]^2. \quad (33)$$

It does not depend on l and can be represented as an integral over three momenta

$$B = (1/(2\pi)^4 l) \int d^2q d^2p d^2p' \frac{|l/2 + q|(q+p)(q+p')(l+p_+ - p_-)(l+p'_+ - p'_-)}{p_+ p_- p'_+ p'_- |q+p|^3 |q+p'|^3}, \quad (34)$$

where

$$p_\pm = |p \pm l/2|, \quad p'_\pm = |p' \pm l/2|. \quad (35)$$

It is a well-defined integral. Calculations give

$$B = 1.962 \pm 0.002.$$

The remaining problem is to separate the PP cross-section from the absorptive part D .

3 The pomeron-pomeron cross-section

To separate the PP cross-section from the absorptive part for central diffractive events we compare the latter with the elastic amplitude $A(s, t)$ for the scattering of the projectile and target in the same approach. In the single pomeron exchange approximation we have

$$A(s, t) = ig^4 (N^2 - 1) s \int d^2r d^2r' \rho_1(l, r) \rho_2(-l, r') G_l(s, r, r'). \quad (36)$$

The normalization is chosen to have the elastic cross-section

$$d\sigma^{el}/dt = (1/16\pi s^2)|A(s, t)|^2. \quad (37)$$

Performing calculations similar to which lead us to Eq. (32) we find for the forward scattering $t = 0$

$$A(s, 0) = i \frac{2}{(2\pi)^2} g^4 (N^2 - 1) s^{1+\Delta} R_1 R_2 \sqrt{\frac{\pi}{a \ln s}} \quad (38)$$

and for $t < 0$

$$A(s, t) = i \frac{2}{(2\pi)^2} g^4 (N^2 - 1) s^{1+\Delta} R_1 R_2 F_1(t) F_2(t) \frac{\sqrt{\pi}}{(a \ln s)^{3/2}}. \quad (39)$$

Evidently one cannot determine the pomeron and its couplings in a unique way from these expressions. One also notices that the amplitude at $t = 0$ rises with s faster than at $t < 0$ by a factor $\ln s$. This shows that the amplitude has a discontinuous behaviour at $t = 0$, which results in the logarithmic singularity of the form-factors $F_{1,2}(t)$ at $t = 0$. As a consequence we meet with an additional difficulty in fixing the "flux factor", since working at $t < 0$, we cannot fix the coupling by its value at $t = 0$.

Therefore rather to fix the flux factor from the coupling, we choose a particular expression for the pomeron propagator, which simplifies the factor entering the triple pomeron vertex. We take that the pomeron contribution is at $t = 0$

$$P(s, 0) = 2\sqrt{\pi} \frac{s^{1+\Delta}}{\sqrt{a \ln s}} \quad (40)$$

and at $t < 0$

$$P(s, t) = 4\sqrt{\pi} \frac{s^{1+\Delta}}{(a \ln s)^{3/2}}. \quad (41)$$

Then we find for its coupling γ to a real external particle at $t = 0$

$$\gamma(0) = \frac{1}{2\pi} g^2 \sqrt{N^2 - 1} R \quad (42)$$

and at $t < 0$

$$\gamma(t) = \frac{1}{2\pi\sqrt{2}} g^2 \sqrt{N^2 - 1} R F(t). \quad (43)$$

These expressions define the flux factor in our case. Of course, they are not unique: one can always multiply the coupling by a constant, simultaneously dividing the propagator by its square.

Rewriting (32) in terms of these quantities we obtain

$$D = M^2 \gamma_1^2(t_1) \gamma_2^2(t_2) P^2(s_1, t_1) P^2(s_2, t_2) \sigma_{PP}^{tot}(M^2, t_1, t_2), \quad (44)$$

where the PP total cross-section, defined by this equation, is

$$\sigma_{PP}^{tot}(M^2, t_1, t_2) = 2\pi^{-7/2} g^8 \frac{N^4}{N^2 - 1} \frac{M^{2\Delta}}{\sqrt{a \ln M^2}} \frac{B^2}{\sqrt{t_1 t_2}}. \quad (45)$$

Evidently it has the form (1) indicated in the Introduction on general grounds, with the constant factor c given by

$$c = 512\sqrt{\pi} \frac{N^4}{N^2 - 1} B^2 \simeq 35370. \quad (46)$$

Note that the PP cross-section can be written in terms of the triple-pomeron vertex $\gamma_{3P}(t)$ found in [1] to be (with the flux factor given by Eqs. (40)-(43))

$$\gamma_{3P}(t) = \frac{g^4 N^2 B}{\pi^2 \sqrt{N^2 - 1}} \frac{1}{\sqrt{-t}}. \quad (47)$$

In terms of γ_{3P} and the pomeron propagator at $t = 0$ (40) the PP cross-section (45) reads

$$\sigma_{PP}^{tot}(M^2, t_1, t_2) = \gamma_{3P}(t_1) \gamma_{3P}(t_2) P(M^2, 0) / M^2. \quad (48)$$

Thus the pomeron-pomeron interaction correctly factorizes into a pair of triple pomeron vertices joined by a pomeron which propagates between them (this fact is independent of the normalization of the pomeron propagators in Eqs. (40) and (41)). The characteristic $1/\sqrt{t_1 t_2}$ behaviour of the cross-section follows that of the two triple pomeron vertices.

4 Discussion

The obtained result corresponds to an exact prediction of the hard pomeron theory, within the mentioned uncertainties associated with the choice of scale in logarithmic factors. To relate these results to observable data one has to specify the range of transferred momenta to which they may apply and the value of the fixed coupling constant α_s . The transferred momenta should not evidently be too low, to avoid confinement effects neglected in the hard pomeron theory. So one should take at least $|t_{1,2}| > 1$ (GeV/c)² and higher values of $|t_{1,2}|$ would be preferable.

As to the coupling constant α_s , it may naively be identified with the expected value of the running QCD coupling constant at the appropriate scale defined by the values of $|t_{1,2}|$. However assuming that α_{QCD} is around 0.2 at 1 GeV/c, one arrives at the well-known value of the intercept $\Delta \sim 0.5$, which not only contradicts soft scattering data but is also about twice larger than the intercept observed in low- x DIS data, performed at comparable values of the momentum transfer [8]. For this reason we prefer to treat α_s as a free parameter inherent in the hard pomeron theory, whose values can be deduced from the observed intercepts determined at appropriate momentum transfers. Low- x DIS experiments at relatively small momentum transfers give the value of the intercept $\Delta \simeq 0.19$ [8]. From this, using (18) we deduce

$$\alpha_s = 0.072. \quad (49)$$

With this value of α_s and at $|t_{1,2}| = 1$ (GeV/c)² we get for the triple pomeron vertex (Eq. (47))

$$\gamma_{3P}(|t| = 1 \text{ (GeV/c)}^2) = 0.32 \text{ mb}^{1/2} \quad (50)$$

and for the PP total cross-section

$$\sigma_{PP}^{tot}(s, |t_{1,2}| = 1 \text{ (GeV/c)}^2) = 0.34 \frac{s^{0.19}}{\sqrt{\ln s}} \text{ mb}. \quad (51)$$

In the latter formula we assume that the appropriate scale is around 1 GeV, so that s should be measured in GeV². At $\sqrt{s} = 6$ TeV from (51) we get the PP cross-section 2.2 mb.

Comparing to the existing phenomenological estimates, based on diffractive scattering data, we observe that the value of the triple pomeron vertex (50) is quite close to the one obtained from the lower energy and t data $\gamma_{3P} = 0.364 \pm 0.025 \text{ mb}^{1/2}$ [9]. The experimental value actually refers to quite small $|t| \sim 0.05 \text{ (GeV/c)}^2$. Our theoretical value obtained for much higher $|t|$ is only slightly smaller, which seem to indicate that the triple pomeron interaction freezes at $|t|$ of the order of 1 (GeV/c)², where the confinement effects are expected to set in.

As a result, our predictions of the PP cross-section are of the same order as the estimates done in [10] on the basis of the experimental value for the triple pomeron vertex. In this reference values of σ_{PP} for the PP c.m. energy intervals $2 \div 180$ and $2 \div 600$ GeV were estimated to be 0.3 mb and 0.6 mb, respectively. Our Eq. (51) gives $\sigma_{PP} = 0.37$ mb for $\sqrt{s} = 2$ GeV and 1.08 mb for $\sqrt{s} = 600$ GeV.

One should have in mind that the magnitude of the PP cross-section is very sensitive to the choice of α_s and the resulting values of the intercept Δ . Taking $\alpha = 0.1$, only slightly larger than (49), raises the intercept to $\Delta = 0.265$, with a consequence that the PP cross-section at $\sqrt{s} = 6$ TeV and $|t_{1,2}| = 1 \text{ (GeV/c)}^2$ rises more than 10 times to achieve values around 30 mb! For the range of energies considered in [10] we would then obtain PP cross-sections between 1.3 mb (at 2 GeV) and 9 mb (at 600 GeV). Therefore the experimental study of the PP cross-section presents a very efficient and sensitive test for possible signatures of the hard pomeron physics.

5 Acknowledgements

The authors express their deep gratitude to Prof. C.Pajares for illuminating discussions. N.A. and M.A.B. thank the CICYT of Spain and IBERDROLA, respectively, for financial support. M.A.B. is also grateful to INTAS, which partly supported this study under the project INTAS 93-79.

6 References

- [1] M.A.Braun, St. Petersburg University preprint SPbU-IP-1995/10 (hep-ph/9506245) (to be published in *Z. Phys. C*).
- [2] V.S.Fadin, E.A.Kuraev and L.N.Lipatov, *Phys. Lett.* **B60** (1975) 50; I.I.Balitsky and L.N.Lipatov, *Sov. J. Nucl. Phys.* **15** (1978) 438.
- [3] A.Donnachie and P.V.Landshoff, *Nucl. Phys.* **B244** (1984) 322; E.L.Berger, J.C.Collins, D.E.Soper and G.Sterman, *Nucl. Phys.* **B286** (1987) 704; K.Goulianos, *Phys. Rep.* **101** (1983) 169.
- [4] J.Bartels, *Nucl. Phys.* **B175** (1980) 365.
- [5] L.N.Lipatov, *Zh. Eksp. Teor. Fiz.* **90** (1986) 1536 (*Sov. Phys. JETP* **63** (1986) 904).
- [6] N.N.Nikolaev and B.G.Zakharov, *Z. Phys.* **C49** (1991) 607.
- [7] A.H.Mueller and W.-K.Tang, *Phys. Lett.* **B284** (1992) 123.
- [8] H1 Collaboration, S.Aid et al, preprint DESY 96-039 (hep-ex/9603004) (submitted to *Nucl. Phys. B*).
- [9] R.L.Cool et al, *Phys. Rev. Lett.* **47** (1981) 701.
- [10] K.H.Streng, *Phys. Lett.* **B166** (1986) 443; R.Engel, M.A.Braun, C.Pajares and J.Ranft, Santiago preprint US-FT/18-96, Siegen preprint SI 96-04 (hep-ph/9605227) (submitted to *Z. Phys. C*).

Figure captions

Fig. 1. Diagram corresponding to the absorptive part for central diffractive events in hadronic (photonic) interactions. Ladders show pomerons emitted by the projectile and target.

Fig. 2. The central part of the diagram of Fig. 1. The upper and lower pomerons are joined to the central one via two Bartels' vertices.

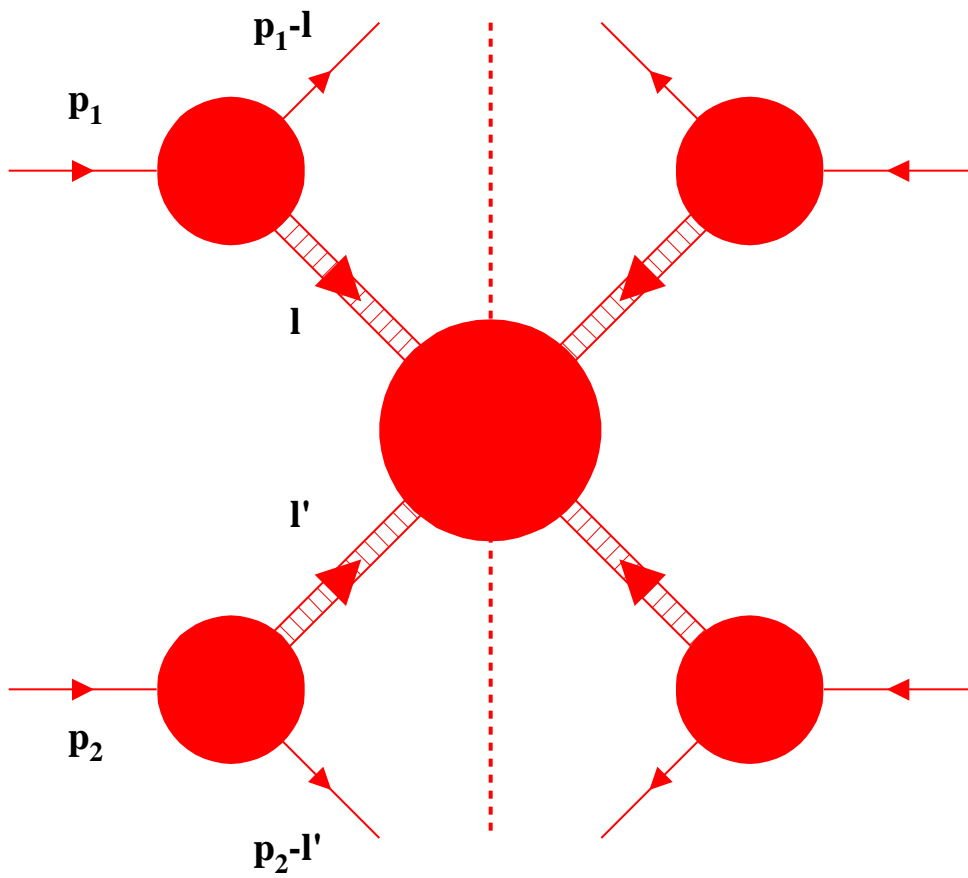


Fig. 1

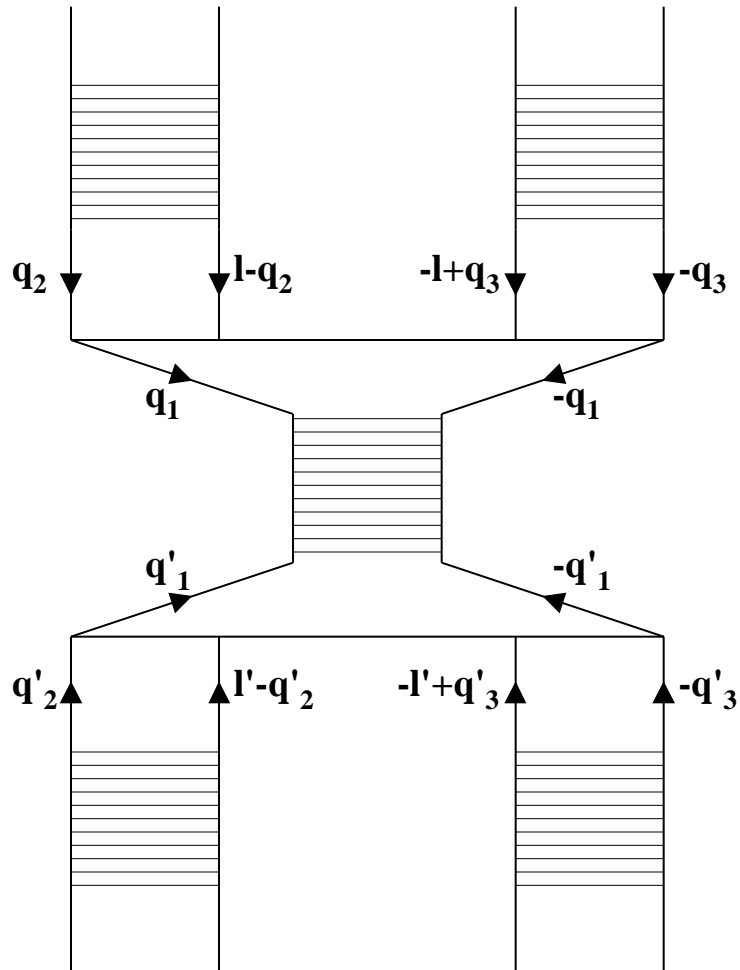


Fig. 2